Nesting, Spin Fluctuations, and Odd-Gap Superconductivity in $Na_xCoO_2 \cdot yH_2O$

M. D. Johannes, I. I. Mazin, D. J. Singh, and D. A. Papaconstantopoulos
Code 6391, Naval Research Laboratory, Washington, D.C. 20375 USA
(Received 3 March 2004; published 27 August 2004)

We calculated the one-electron susceptibility of hydrated Na_xCoO_2 and find strong nesting, involving about 70% of all electrons at the Fermi level and nearly commensurate with a 2×2 superstructure. This nesting creates a tendency to a charge density wave compatible with the charge order often seen at $x \approx 0.5$ and usually ascribed to electrostatic repulsion of Na ions. In the spin channel, it leads to strong spin fluctuations, which should be important for superconductivity. The state most compatible with this nesting structure is an odd-gap triplet s-wave state.

DOI: 10.1103/PhysRevLett.93.097005 PACS numbers: 74.20.–z

The discovery of superconductivity in the layered oxide $Na_{1/3}CoO_2 \cdot 1.4H_2O$ is the subject of intense research despite its relatively low critical temperature. This is due to properties that suggest a nontrivial superconducting state and/or a nontrivial pairing mechanism. These include unusual magnetic, thermodynamic, and transport properties, the apparent proximity to both structural and magnetic instabilities, and the frustrated triangular Co lattice .

A variety of possible pairing interactions may be relevant in this system. Structural instabilities have been reported in the nonhydrated compound [4,7], suggesting the possibility of a related soft mode and thus strong electron-phonon coupling. A high polarizability of water suggests the old proposal of "sandwich" superconductivity, where the attraction between electrons in metallic layers is mediated by dynamic excitations in the highly polarizable layers [8]. Local density approximation (LDA) calculations yield a ferromagnetic ground state [9,10]; an antiferromagnetic solution is slightly higher in energy but still favored over the nonmagnetic state, presaging long-range spin fluctuations that are observed at some dopings [11]. Finally, and this is the central point of the current Letter, nesting properties of the Fermi surface (FS) suggest strong antiferromagnetic spin fluctuations, which are bound to play an important role in superconductivity (as well as in the normal transport). First and foremost, they make a conventional singlet s-wave state rather unlikely.

Experimental evidence for a pairing symmetry is still inconclusive. Some Knight shift data suggest a triplet state with order parameter directed out of the plane [12–14]. Nonexponential behavior below T_c was observed in muon spin relaxation (μSR), nuclear magnetic resonance (NMR), and nuclear quadrupole resonance (NQR) experiments [15,16], inconsistent with a fully gapped state; some reported a coherence peak maximum near T_c [14,17], while others did not find it, possibly because of impurity scattering.

Here we calculate the one-electron susceptibility and show that it has strong structure in reciprocal space, which is not related to crystal symmetry but is, accidentally, nearly commensurate with the lattice. This structure is robust with respect to doping and interlayer distance and may even be responsible for the reported superstructures (as opposed to an intuitive picture relating them solely to Coulomb ordering of Na ions). The calculated spin fluctuations are pair breaking for either singlet or triplet BCS superconductivity, but they are fully compatible with so-called odd-gap superconductivity, the most favorable symmetry being triplet s wave.

The strength of Coulomb correlations in $Na_{1/3}CoO_2 \cdot 1.4H_2O$ (subsequently called NCO) is yet unknown, but even in metals as strongly correlated as the high-T_c cuprates, LDA calculations consistently provide accurate FSs. The one-electron bands of the parent, Na_xCoO_2, are now well understood [9,18]. The Co d bands are split by the octahedral crystal field into three t_{2g} bands per layer, well separated from the two e_g bands. The former further split in the hexagonal symmetry into one a_{1g} and two e'_g bands. The a_{1g} and one of the two e'_g bands cross the Fermi level, forming, respectively, a large hexagonal hole pocket around the Γ point and six small, elliptical hole pockets [19]. The effect of hydration on the electronic structure has been shown to be, for all practical purposes, related solely to lattice expansion [22], and we will therefore use an unhydrated but expanded compound for our calculations. The neglected effects of Na or H_2O disorder would, if anything, further enhance two dimensionality.

We made a tight-binding (TB) fit to our paramagnetic full-potential linearized augmented plane wave (LAPW) [23] band structure near E_F. The bond length dependence of the TB parameters was incorporated as described in Ref. [24] and was used to analyze FS dependence on the interlayer distance c with the O ion at its relaxed position in the hydrated compound. The fits (details to be published elsewhere [25]) have an rms error of three mRy in the relevant energy range. This accuracy and a mesh of over 30 000 k points in the Brillouin zone were needed for good resolution of the small FS pockets. We used the fit to calculate the one-electron susceptibility $\chi_0(\mathbf{q}, \omega) = \chi'_0(\mathbf{q}, \omega) + i\chi''_0(\mathbf{q}, \omega)$:

$$\chi_0(\mathbf{q}, \omega) = \sum_{\mathbf{k}} [f(\epsilon_{\mathbf{k}+\mathbf{q}}) - f(\epsilon_{\mathbf{k}})]/(\epsilon_{\mathbf{k}} - \epsilon_{\mathbf{k}+\mathbf{q}} - \omega - i\delta),$$

where $\epsilon_{\mathbf{k}}$ is the one-electron energy, f is the Fermi function, and the matrix elements are neglected [26]. The results reported below are for $x = 0.03$, but the described nesting features remain up to at least $x = 0.05$. Figure 3 shows the nesting structure in $\chi_0''(\mathbf{q}, \omega)/\omega$ at $\omega \to 0$, important for superconductivity, and also in $\chi_0'(\mathbf{q}, 0)$.

With an increased c, as expected, the bands are completely two-dimensional within the accuracy of our calculations. The $e_{g'}$ holes get heavier and comprise $\sim 70\%$ of the density of states at the Fermi energy (Fig. 1), though the total volume of these pockets is half the volume of the a_{1g} pocket. The latter, which was a hexagonal prism with moderately flat faces in the parent compound, becomes nearly circular and, hence, its contribution to the susceptibility is practically featureless. However, the six elliptical pockets are well nested and, because of two dimensionality, their small size can only enhance the susceptibility at the nesting vector, leaving the deviation from circular cylindrical shape as the only factor determining nesting strength. Indeed, if they were exactly circular, all three nesting vectors $\mathbf{Q_1}$, $\mathbf{Q_2}$, and $\mathbf{Q_3}$, shown in Fig. 2 by solid, narrow dashed, and wide dashed lines, respectively, would nest perfectly. No symmetry requirement forces these pockets to be circular nor is there a restriction imposed on their distance from the Γ point. However, due to their small size they are nearly perfectly elliptical so that, for example, pockets A and D in Fig. 2 nest nearly exactly, and, accidentally, the distance between them is just slightly less than half of the reciprocal lattice vector $\mathbf{G}$. As a result, a strong double-humped peak appears in the calculated χ_0'' (Fig. 3) at all $\mathbf{G}/2$.

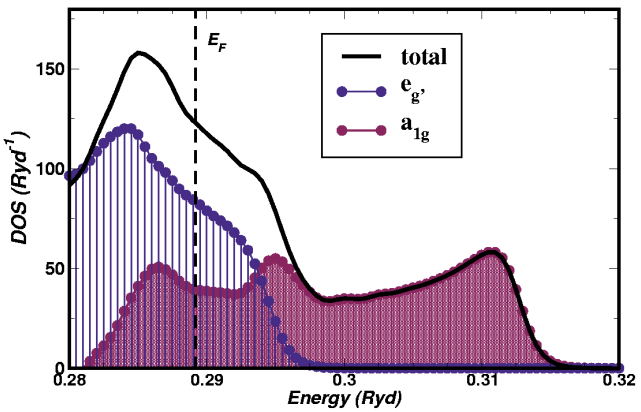

FIG. 1 (color online). (color online) The density of states of $Na_{0.3}CoO_2 \cdot yH_2O$ and of the two bands crossing the Fermi level. The a_{1g} band, which carries 2/3 of all holes, yields only about 1/3 of $N(E_F)$.

Since $\mathbf{Q_1} \approx \mathbf{G}/2$, $\mathbf{Q_2}$ and $\mathbf{Q_3}$ are close to $\mathbf{G}/4$, as seen in Fig. 3. The corresponding peaks are suppressed by the ellipticity of the $e_{g'}$ pockets, which creates misorientation between the pockets A and B or A and C. As long as the pockets are perfect ellipses, the peaks at $\mathbf{Q_2}$ and $\mathbf{Q_3}$ have the same amplitude. In the real part of χ the peak at $\mathbf{Q_1}$ is broadened but still prominent, while the peaks at $\mathbf{Q_2}$, $\mathbf{Q_3}$ are smeared out.

Thus there is prominent nesting structure in both real and imaginary parts of χ_0 at all half-integer reciprocal lattice coordinates and weaker but noticeable structure at all quarter-integer coordinates in χ_0''. Because of two dimensionality [27], in the charge channel this structure can lead to a Peierls-type charge density wave instability, i.e., a structural transition. Indeed, various superstructures have been reported, especially at $x = 1/2$, and are often ascribed to charge ordering of Na ions. Our results suggest that the CoO_2 planes themselves have a tendency toward superstructure formation, even without Na ordering. The observed superstructures, presumably, are affected by both factors. Finally, there are indications [4,7] that an antiferromagnetic ordering may set in parallel to a structural instability, which in our picture would correspond to the condensation of a spin density wave at a nesting vector.

At the compositions where the structure in χ' does *not* lead to an instability, one may expect soft modes associated with the corresponding wave vectors. However, for superconductivity, the corresponding spin fluctuations, which take advantage not only of the structure in χ_0' but also of the (much sharper) structure of χ_0'', are more interesting. Let us first concentrate on the strongest peak in χ_0'', at $\mathbf{q}=\mathbf{Q}_1$, and consider possible signs of the order parameter on the corresponding pockets (A and D in Fig. 2). The relevant part of the linearized equation for the order parameter can be written as

$$\Delta(\mathbf{k}_A, i\omega_n) = T\sum_{\omega_n'} \frac{V(\mathbf{Q}_1, i\omega_n - i\omega_n')}{\xi_{\mathbf{k}_D}^2 + |\omega_n'|^2} \Delta(\mathbf{k}_D, i\omega_n'). \quad (1)$$

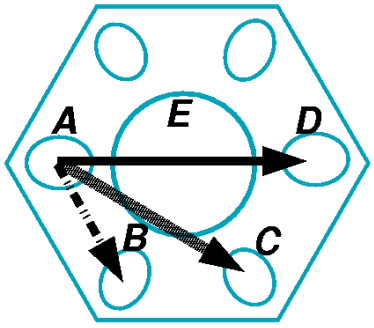

FIG. 2 (color online). The three main nesting types in $Na_{0.3}CoO_2 \cdot yH_2O$. The perfect nesting at $\mathbf{Q_1}$ is shown as a solid line and the two imperfect, $\mathbf{Q_2}$ and $\mathbf{Q_3}$, in narrow and wide dashed lines.

The order parameter Δ is scalar for singlet and vector for triplet pairing. The summation includes all Matsubara frequencies ω_n; $\xi_{\mathbf{k}}$ are the quasiparticle energies and $V(\mathbf{q})$ is the pairing potential (positive for attraction). For pairing induced by phonons, $V(\mathbf{q})$ is always positive; for spin fluctuations it is positive for triplet pairing and negative for singlet. Since the pockets A and D are related by spatial inversion, for inversion symmetric order parameters, s, d, etc., a solution to Eq. (1) exists only if $V(\mathbf{Q}_1) > 0$, that is, in the triplet channel, and for antisymmetric order parameters, p, etc., only in the singlet channel. Note that such strict selection rules are related to the small size of the e'_g pockets. Nesting in a large FS that can support line nodes can, in principle, induce a singlet d-wave state, as discussed, e.g., in Ref. [28].

The Pauli principle forbids both singlet-p (Sp) and triplet-s (Ts) states, as well as Td, unless the order parameter is odd with respect to frequency, as discussed by Berezinskii [29] for He^3 and in the context of solid state by by Rieck *et al.* and by Balatsky and collaborators [30]. In other words, spin fluctuations with $\mathbf{q}=\mathbf{Q}_1$ are pairing for the odd-gap Sp state (oSp) and for the odd-gap Ts state (oTs). The relative stability of these must be decided by other interactions. Staying within the spin-fluctuation scenario, we include now the two other nesting vectors, $\mathbf{Q}_2$ and $\mathbf{Q}_3$. Let us first consider the oS state.

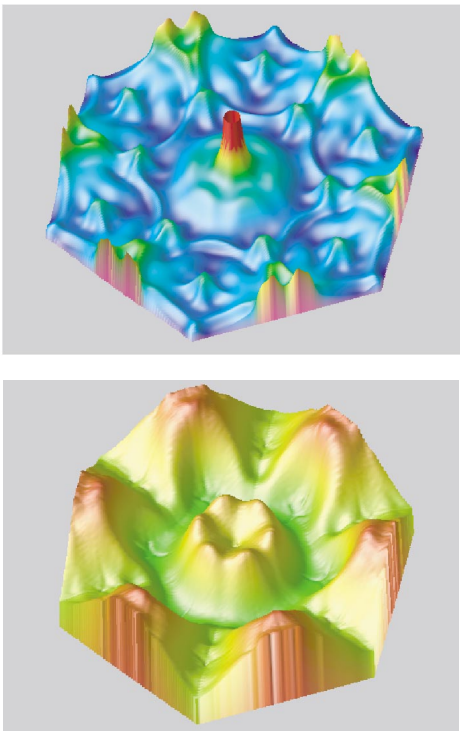

FIG. 3 (color online). (color online) (top) $\lim_{\omega\to 0}\chi_0''(\mathbf{q},\omega)/\omega$ The double-humped peaks corresponding to $\mathbf{Q_1}$ nesting appear along the flat edges of the zone boundary. (bottom) $\chi_0'(\mathbf{q}, 0)$. A temperature broadening of 1 mRy was used.

The order parameter is a scalar, which we assume to be constant within each of the pockets, with a phase changing from pocket to pocket (Fig. 4). The lowest angular momentum solution allowed for a real order parameter corresponds to an f wave, changing among the pockets as $\Delta_A \tilde{a}\tilde{N}\ \Delta_B \tilde{a}\tilde{N}\ \Delta_C \tilde{a}\tilde{N}\ \Delta_D = 1\tilde{a}\tilde{N}\ -1\tilde{a}\tilde{N}\ 1\tilde{a}\tilde{N}\ -1$, which implies several node lines in the induced gap on the pocket E. A complex p-wave order parameter is also allowed, so that $\Delta_A \tilde{a}\tilde{N}\ \Delta_B \tilde{a}\tilde{N}\ \Delta_C \tilde{a}\tilde{N}\ \Delta_D = 1\tilde{a}\tilde{N}\ e^{i\pi/3}\tilde{a}\tilde{N}\ e^{2i\pi/3}\tilde{a}\tilde{N}\ -1$. In this case, the induced order parameter on the pocket E varies with angle as $e^{i\phi}$ and is nodeless, thus energetically more favorable. Note that as long as the spin fluctuations with vectors $\mathbf{Q}_2$ and $\mathbf{Q}_3$ couple to electrons with equal strength, they do not contribute to pairing at all in either case, canceling each other completely (because of the phase factor). The oTs state can actually benefit from both "minor" nestings. In this case, there are no symmetry-implied nodes, and the simplest solution has constant gaps over both types of FSs. The order parameters are now spinors, which can be translated in a standard way into real-space vectors. Several solutions are possible with pair spins either in or perpendicular to the hexagonal plane, for instance, $\mathbf{d} = \text{const} \cdot \hat{\mathbf{z}}$, where $\hat{\mathbf{z}}$ is the unit vector in c direction, or $\mathbf{d} = \text{const} \cdot (\hat{\mathbf{x}} + i\hat{\mathbf{y}})$. Importantly, for any of the oTs states, all spin fluctuations are pairing, including those with $\mathbf{q}=\mathbf{Q}_2$ and $\mathbf{q}=\mathbf{Q}_3$. Furthermore, an oTs state seems compatible with the limited experimental information available on the pairing symmetry. First, such a state would not exhibit exponential behavior in such experiments as specific heat, NMR/NQR, and penetration depth [15,16]. Second, the coherence peak should be suppressed compared to a conventional eSs state. (In most experiments such a peak is not observed, but a rather weak coherence peak was seen in Refs. [14,17]). Third, specifically the $\mathbf{d} \parallel \hat{\mathbf{z}}$ triplet s state, similar to the chiral p state

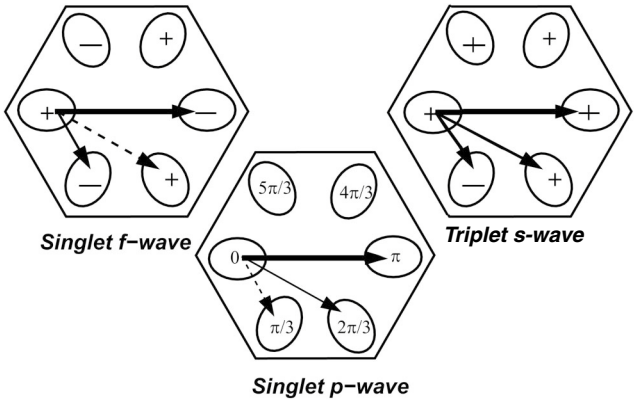

FIG. 4. The order parameter phase on the relevant sheets of the FS of various odd-gap superconducting states in NCO. Solid black lines indicate pairing interactions and dashed lines, pair breaking. In the central panel, the phase factors are $e^{i\delta}$ where δ is indicated in each pocket.

in Sr_2RuO_4 implies no change in the in-plane susceptibility, as measured by the Knight shift. [12–14]. Finally, nonmagnetic impurities are not pair breaking for an oTs state, in agreement with observation [31].

The odd-gap superconducting state is gapless; therefore other pairing symmetries, if possible, have an energetic advantage. However, not only are these spin fluctuations pairing in the oTs (and to a lesser extent, in the oSp) symmetry, but are strongly pair breaking for all other superconducting symmetries. Therefore, even if other interactions favor more conventional superconducting states, the choice between possible symmetries must include the pair breaking effects from these fluctuations. Finally, although the a_{1g} FS is without pronounced nesting, it will couple to these same spin fluctuations, as both sheets are derived from Co d orbitals. This FS yields $\sim$ 30% of the total density of states, so a more quantitative theory should take into account possible pairing or pair breaking effects on this FS as well.

We acknowledge valuable discussions with A. Balatsky, D. Mandrus, S. Nagler, B. Sales, and K. Scharnberg. We are particularly grateful to D. Agterberg for pointing out to us the possibility of odd-gap superconductivity in connection with the nesting in this compound.

[1] I. Terasaki, Y. Sasago, and K. Uchinokura, Phys. Rev. B **56**, 12685 (1997).
[2] Y. Y. Wang *et al.*, Nature **423**, 425 (2003).
[3] Y. Ando *et al.*, Phys. Rev. B **60**, 10580 (1999).
[4] Q. Huang *et al.*, cond-mat/0402255 (2004).
[5] G. Baskaran, Phys. Rev. Lett. **91**, 097003 (2003).
[6] S. Y. Li *et al.*, Phys. Rev. Lett. **93**, 056401 (2004).
[7] B. C. Sales *et al.*, cond-mat/0402379 (2004).
[8] D. Allender, J. Bray, and J. Bardeen, Phys. Rev. B **7**, 1020 (1973).
[9] D. J. Singh, Phys. Rev. B **61**, 13397 (2000).
[10] D. J. Singh, Phys. Rev. B **68**, 020503 (2003).
[11] A. T. Boothroyd *et al.*, cond-mat/0312589 (2003).
[12] W. Higemoto *et al.*, cond-mat/0310324 (2003).
[13] A. Kanigel *et al.*, cond-mat/0311427 (2003).
[14] T. Waki *et al.*, cond-mat/0306036 (2003).
[15] T. Fujimoto *et al.*, Phys. Rev. Lett. **92**, 047004 (2004).
[16] K. Ishida *et al.*, J. Phys. Soc. Jpn. **72**, 3041 (2003).
[17] Y. Kobayashi, M. Yokoi, and M. Sato, J. Phys. Soc. Jpn. **72**, 2453 (2003).
[18] K.-W. Lee, J. Kunes, and W. E. Pickett, Phys. Rev. B **70**, 045104 (2004).
[19] While the larger FS has already been observed by photoemission experiments [20,21], no evidence of these hole pockets has been found so far. However, both experiments have been performed at a much higher doping level where, as mentioned, the physical properties of Na_xCoO_2 are qualitatively different. The ability of LDA to predict FSs is well established by examples such as Sr_2RuO_4 and the strongly correlated $YBa_2Cu_3O_7$. In both of these cases, initial disagreement between LDA predictions and photoemission was eventually resolved in favor of LDA. Specifically, the FS of Sr_2RuO_4 is formed by the same three t_{2g} orbitals as in Na_xCoO_2, and its topology is also determined by fine details of the crystal field splitting between different t_{2g}-derived bands. It is reasonable to assume that LDA predictions will be similarly successful for the cobaltate compound. The ultimate answer should be given by bulk quantum oscillation experiments.
[20] M. Z. Hasan *et al.*, Phys. Rev. Lett. **92**, 246402 (2004).
[21] H.-B. Yang *et al.*, Phys. Rev. Lett. **92**, 246403 (2004).
[22] M. D. Johannes and D. J. Singh, Phys. Rev. B **70**, 014507 (2004).
[23] P. Blaha *et al.*, *Wien2k, an Augmented Plane Wave + Local Orbitals Program for Calculating Crystal Properties* (Karlheinz Schwarz, Technical University of Wien, Vienna, 2002), ISBN 3-9501031-1-2.
[24] D. A. Papaconstantopoulos and M. J. Mehl, J. Phys. Condens. Matter **15**, R413 (2003).
[25] M. D. Johannes *et al.*, Euro. Phys. Lett. (to be published).
[26] This approximation is good as long as the character of the wave functions at $\mathbf{k}$ and $\mathbf{k}+\mathbf{q}$ is the same. This is true for a_{1g} transitions and the$\mathbf{Q_1}$ nesting. Because of the double degeneracy of the $e_{g'}$ representation, the matrix elements will be reduced for $\mathbf{Q_2}$ and $\mathbf{Q_3}$ by a factor of up to two and suppressed for the weakly structured $a_{1g} - e_{g'}$ component. For the qualitative discussion here, the constant matrix elements approximation is sufficient.
[27] Figure 3 applies to hydrated NCO with $x = 0.3$. Unhydrated NCO is less two-dimensional and even less as x increases. However, we expect the unhydrated compound to have similar nesting properties, albeit less pronounced.
[28] Y. Fuseya, H. Kohno, and K. Miyake, J. Phys. Soc. Jpn. **72**, 2914 (2003).
[29] V. L. Berezinskii, JETP Lett. **20**, 287 (1974).
[30] C. T. Rieck, K. Scharnberg, and N. Schopohl, J. Low Temp. Phys., **84**, 381 (1991); A. Balatsky and E. Abrahams, Phys. Rev. B **45**, 13125 (1992).
[31] M. Yokoi *et al.*, cond-mat/0312242 (2003).